

# All-optical link for direct comparison of distant optical clocks

Miho Fujieda<sup>1</sup>, Motohiro Kumagai<sup>1</sup>, Shigeo Nagano<sup>1</sup>,  
Atsushi Yamaguchi<sup>1,2</sup>, Hidekazu Hachisu<sup>1,2</sup>, and Tetsuya Ido<sup>1,2</sup>

<sup>1</sup>National Institute of Information and Communications Technology,  
4-2-1, Nukui-kitamachi, Koganei, Tokyo, 184-8795 Japan

<sup>2</sup>CREST, Japan Science and Technology Agency,  
4-1-8, Honcho, Kawaguchi, Saitama, 332-0012 Japan

[miho@nict.go.jp](mailto:miho@nict.go.jp)

**Abstract:** We developed an all-optical link system for making remote comparisons of two distant ultra-stable optical clocks. An optical carrier transfer system based on a fiber interferometer was employed to compensate the phase noise accumulated during the propagation through a fiber link. Transfer stabilities of  $2 \times 10^{-15}$  at 1 second and  $4 \times 10^{-18}$  at 1000 seconds were achieved in a 90-km link. An active polarization control system was additionally introduced to maintain the transmitted light in an adequate polarization, and consequently, a stable and reliable comparison was accomplished. The instabilities of the all-optical link system, including those of the erbium doped fiber amplifiers (EDFAs) which are free from phase-noise compensation, were below  $2 \times 10^{-15}$  at 1 second and  $7 \times 10^{-17}$  at 1000 seconds. The system was available for the direct comparison of two distant  $^{87}\text{Sr}$  lattice clocks via an urban fiber link of 60 km. This technique will be essential for the measuring the reproducibility of optical frequency standards.

© 2022 Optical Society of America

**OCIS codes:** (120.3940) Metrology; (060.2360) Fiber optics links and subsystems; (120.4800) Optical standards and testing.

---

## References and links

1. G. Panfilo and E. Felicitas Arias, "Algorithms for International Atomic Time," *IEEE Trans. Ultrason. Ferroelectr. Freq. Control* **57**(1), 140-150 (2010).
2. C. W. Chou, D. B. Hume, J. C. J. Koelemeij, D. J. Wineland, and T. Rosenband, "Frequency comparison of Two High-Accuracy  $\text{Al}^+$  Optical Clocks," *Phys. Rev. Lett.* **104**, 070802 (2010).
3. S. M. Foreman, K. W. Holman, D. D. Hudson, D. J. Jones, and J. Ye, "Remote transfer of ultrastable frequency references via fiber networks," *Rev. Sci. Instr.* **78**, 021101 (2007).
4. P. A. Williams, W. C. Swann, N. R. Newbury, "High-stability transfer of an optical frequency over long fiber-optic links," *J. Opt. Soc. Am. B* **25**(8), 1284-1293 (2008).
5. M. Musha, F.-L. Hong, K. Nakagawa, K. Ueda, "Coherent optical frequency transfer over 50-km physical distance using a 120-km-long installed telecom fiber network," *Opt. Exp.* **16**(21), 16459-16466 (2008).
6. L. S. Ma, P. Jungner, J. Ye, and J. L. Hall, "Delivering the same optical frequency at two places: accurate cancellation of phase noise introduced by an optical fiber or other time-varying path," *Opt. Lett.* **19**(21), 1777-1779 (1994).
7. N. R. Newbury, P. A. Williams, and W. C. Swann, "Coherent transfer of an optical carrier over 251 km," *Opt. Lett.* **32**(21), 3056-3058, 2007.
8. F. Kefelian, O. Lopez, H. Jiang, C. Chardonnet, A. Amy-Klein, G. Santarelli, "High-resolution optical frequency dissemination on a telecommunications network with data traffic," *Opt. Lett.* **34**(10), 1573-1575 (2009).

9. O. Lopez, A. Haboucha, F. Kefelian, H. Jiang, B. Chanteau, V. Roncin, C. Chardonnet, A. Amy-Klein, and G. Santarelli, "Cascaded multiplexed optical link on a telecommunication network for frequency dissemination," *Opt. Exp.* **18**(16), 16849-16857 (2010).
10. O. Terra, G. Grosche, and H. Schnatz, "Brillouin amplification in phase coherent transfer of optical frequencies over 480 km fiber," *Opt. Exp.* **18**(15), 16102-16111 (2010).
11. A. D. Ludlow, T. Zelevinsky, G. K. Campbell, S. Blatt, M. M. Boyd, M. H. G. de Miranda, M. J. Martin, J. W. Thomsen, S. M. Foreman, Jun Ye, T. M. Fortier, J. E. Stalnaker, S. A. Diddams, Y. Le Coq, Z. W. Barber, N. Poli, N. D. Lemke, K. M. Beck, C. W. Oates, "Sr Lattice Clock at  $1 \times 10^{-16}$  Fractional Uncertainty by Remote Optical Evaluation with a Ca clock," *Science* **319**, 1805-1808 (2008).
12. O. Terra, G. Grosche, K. Predehl, R. Holzwarth, T. Legero, U. Sterr, B. Lipphardt, and H. Schnatz, "Phase-coherent comparison of two optical frequency standards over 146 km using a telecommunication fiber link," *Appl. Phys. B* **97**, 541-551 (2009).
13. A. Pape, O. Terra, J. Friebe, M. Riedmann, T. Wubben, E. M. Rasel, K. Predehl, T. Legero, B. Lipphardt, H. Schnatz, and G. Grosche, "Long-distance remote comparison of ultrastable optical frequencies with  $10^{-15}$  instability in fractions of a second," *Opt. Exp.* **18**(20), 21477-21483 (2010).
14. Japan Gigabit Network 2 plus. [Online]. Available: [http://www.jgn.nict.go.jp/jgn2plus\\_archive/english/index.html](http://www.jgn.nict.go.jp/jgn2plus_archive/english/index.html).
15. M. Kumagai, M. Fujieda, S. Nagano, and M. Hosokawa, "Stable radio frequency transfer in 114 km urban optical fiber link," *Opt. Lett.* **34**(19), 2949-2951 (2009).
16. M. Fujieda, M. Kumagai, S. Nagano, "Coherent Microwave Transfer Over a 204-km Telecom Fiber Link by a Cascaded System," *IEEE Trans. Ultrason. Ferroelectr. Freq. Cont.* **57**(1), 168-174 (2010).
17. P. Lesage, "Characterization of frequency stability: bias due to the juxtaposition of time-interval measurements," *IEEE Trans. Instr. Meas.*, **32**(1), 204-207, 1983.
18. M. Takamoto, F. L. Hong, R. Higashi, and H. Katori, "An optical lattice clock," *Nature* **435**, 321-324 (2005).
19. T. Akatsuka, M. Takamoto, and H. Katori, "Optical lattice clocks with non-interacting boson and fermions," *Nature Phys.* **4**, 954 (2008).
20. M. Takamoto, T. Takano, and H. Katori, "Frequency comparison of optical lattice clocks beyond the Dick limit," *Nature Photon* **5**, 288-292 (2011).
21. A. Yamaguchi, M. Fujieda, M. Kumagai, H. Hachisu, S. Nagano, Y. Li, T. Ido, T. Takano, M. Takamoto, and H. Katori, "Direct comparison of distant optical lattice clocks at the  $10^{-16}$  uncertainty," *Appl. Phys. Express*, **4**, 082203 (2011).
22. S. Nagano, H. Ito, Y. Li, K. Matsubara, and M. Hosokawa, "Stable operation of femtosecond laser frequency combs with uncertainty at the  $10^{-17}$  level toward optical frequency standards," *Jpn. J. Appl. Phys.* **48**, 042301 (2009).
23. Y. Y. Jiang, A. D. Ludlow, N. D. Lemke, R. W. Fox, J. A. Sherman, L. S. Ma, and C. W. Oates, "Making optical atomic clocks more stable with  $10^{-16}$ -level laser stabilization," *Nat. Photons* **5**, 158-161 (2011).

---

## 1. Introduction

Clock comparisons are essential to confirm the reproducibility of frequency standards. For the past twenty years, it has been possible to remotely calibrate the frequencies of microwave atomic clocks by using satellite links such as GPS or two-way satellite time and frequency transfer (TWSTFT). One of the applications of these techniques is the network of international atomic time (TAI) links established by Bureau International des Poids et Mesures (BIPM), and it allows us to know time difference between clocks separated by some distance [1]. It is provided by BIPM that today's typical satellite links using GPS precise point positioning and TWSTFT have frequency stabilities of  $1 \times 10^{-15}$  and  $2 \times 10^{-15}$ , respectively, for an averaging time of five days. On the other hand, stabilities of optical frequency standards have rapidly increased, reaching  $1 \times 10^{-16}$  for an averaging time of 1000 seconds [2]. This progress has led to the need for a technique to remotely compare frequencies without degrading their stabilities. However, the frequency stabilities of satellite-based links are apparently insufficient which spoil the benefit of optical standards. Instead, transferring a stable optical frequency over optical fibers is regarded as a strong candidate for making direct comparisons of highly stable optical clocks and, it has been studied extensively [3, 4, 5]. Successful experiments have been performed over a short distance link [6] and with a spooled fiber [7]. Other studies include ones on transfer of a clock signal together with data traffic [8, 9], using a high gain amplifier for a long-haul link up to 480 km [10], and developing a repeater for cascaded systems [9]. Moreover, optical carrier

transfer techniques have been developed to observe the relative frequency stability of optical clocks and cavity stabilized lasers [11, 12, 13]. Stable optical frequency transfer would be useful not only for making frequency comparisons, but also for optical coherent communications.

We developed an all-optical link system that consists of Ti:sapphire (Ti:S) frequency combs, nonlinear crystals for frequency doubling, fiber amplifiers, a  $1.5\ \mu\text{m}$  stable laser, an optical carrier transfer system, and an active polarization control system. The system can perform reliable measurements and can operate for a long time free from large polarization variations caused by the long-haul fiber link. Its feasibility was confirmed in an experiment that directly compared two  $^{87}\text{Sr}$  clocks located at the National Institute of Information and Communications Technology (NICT) and the University of Tokyo (UT). In this paper the details of the system and its performance are described with the result of direct comparison of distant optical clocks.

## 2. Overall system

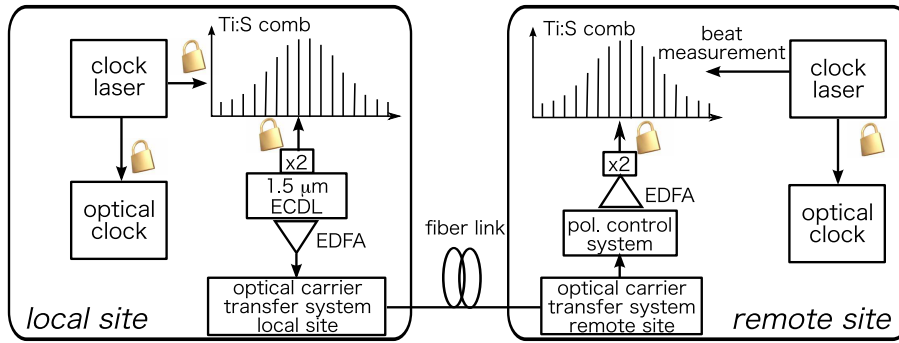


Fig. 1. Overall system of the all-optical link. The clock signal at the local site is frequency-converted into the  $1.5\ \mu\text{m}$  light and transferred to the remote site via an optical fiber link. The optical carrier transfer system compensates the phase noise so that the clock signal is faithfully transferred to the remote site. The transferred light is converted into a visible wavelength to be compared with another clock signal at the remote site. ECDL: external cavity diode laser, x2: PPLN frequency doubler.

Fig. 1 is a diagram of the all-optical link system. A stable optical frequency is sent from the local site to the remote site through an optical fiber link. The telecom wavelength at  $1.5\ \mu\text{m}$  is adequate for transmissions over optical fiber links from the perspective of low optical loss, while most of the optical clock transitions lie in the range of visible light. Hence, there is a need for frequency conversion between the two bands, and the system uses two Ti:S frequency combs and two periodically poled lithium niobate (PPLN) for this purpose. The clock lasers at the both sites are locked to an optical transition of atoms or ions. The Ti:S frequency comb is phase-locked to the clock laser at the local site. An external-cavity diode laser (ECDL) operating at  $1.5\ \mu\text{m}$  is phase-locked to the frequency comb through its second harmonic generation (SHG) light generated by the PPLN. The light emitted from the ECDL is amplified by a booster EDFA and an optical carrier transfer system, which is described below, delivers the light to the remote site. At the remote site, the transferred light is amplified by an EDFA in order to feed enough power into the PPLN there. The state of polarization (SOP) is stabilized by the polarization control system and the light is frequency doubled. The Ti:S frequency comb at the remote site is phase-locked to the SHG light. The beat signal between the clock laser and the nearest comb component represents the differential frequency and the relative stability of the two optical clocks.

### 3. Subsystems

#### 3.1. Optical carrier transfer system

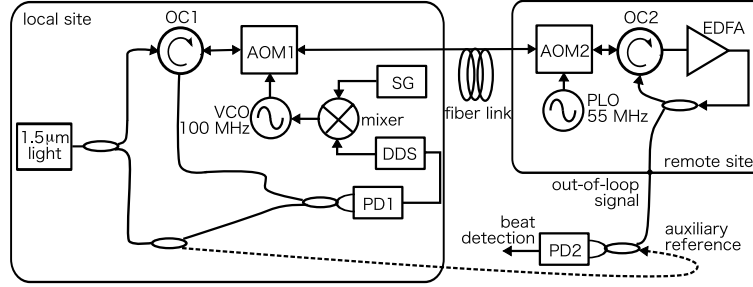


Fig. 2. Schematic diagram of the optical carrier transfer system. The system consists of local and remote parts. To evaluate the system performance, both parts are initially located at the same place. The beat signal between the output of the remote site and auxiliary reference is used for the evaluation. OC: optical circulator, AOM: acousto-optic modulator, VCO: voltage controlled oscillator, SG: signal generator, DDS: direct digital synthesizer, PD: photo detector, PLO: phase locked oscillator, EDFA: erbium doped fiber amplifier.

Fig. 2 shows a schematic diagram of the optical carrier transfer system with which we tested the fiber noise cancellation capability. To compensate the accumulated phase noise during the transmission, we developed a noise cancellation system based on a fiber interferometer. The concept is similar to the scheme demonstrated by Ma et al. [6]. A narrow-bandwidth  $1.5 \mu\text{m}$  light to be transferred is coupled to a fiber-pigtailed acousto-optic modulator 1 (AOM1) driven by a 100-MHz voltage controlled oscillator (VCO) via an optical circulator 1 (OC1) and transmitted to the remote site through a long-haul link. At the remote site, the transmitted light is connected to the second fiber-pigtailed AOM 2 (AOM2) driven by a 55-MHz stable reference and amplified by a uni-directional EDFA. Part of the amplified light is served to a user (denoted as the “out-of-loop signal”), and the rest is sent back to the local site through optical circulator 2 (OC2) and AOM2. AOM2 discriminates the returned signal from the stray reflections at connectors and splices. One concern in using the uni-directional EDFA is that only half of the noise induced by it is compensated by the system. As described later, we found that the remaining half of the noise does not limit the performance of our system. Bi-directional EDFAs and Faraday rotator mirrors (FRMs) are normally used to compensate optical loss and to reflect part of the transmitted light back to the local site. Indeed, the combination of the bi-directional EDFA and the FRM worked properly in performance checks using a spooled fiber or a dedicated fiber link. However, in the case applying a bi-directional EDFA to the fiber link from NICT to UT, unwanted back-reflections from many SC/PC connectors at the remote site induced an excessive amount of input to the bi-directional EDFA, and this resulted in saturation of the output. The returned light to the local site is coupled to a photo detector 1 (PD1) via AOM1 and OC1. AOM1 and AOM2 used  $-1^{\text{st}}$  and  $+1^{\text{st}}$  diffraction, respectively. The frequency of the return light which passes AOM1 and AOM2 twice is shifted by -90 MHz. The polarization change in the traveling light is an important issue in the long-haul link. Retro-reflection by the FRM makes it possible to maintain the difference of the state of polarization (SOP) between the reference and return light. In our case free from the FRM, the return light is differentially detected by a balanced photo detector to moderate the amplitude variation of the 90-MHz beat signal. The obtained beat signal is divided-by-50 to 1.8 MHz by a direct digital synthesizer (DDS). The DDS works not only to expand the capture range of the phase lock for handling of a huge amount of phase noise but also to make the amplitude of the beat signal uniform. The resulting

divided signal is mixed with a 1.8-MHz stable reference linked to a hydrogen maser. The mixer output is amplified, filtered, and fed back to the VCO. Thus, the phase of the VCO is adjusted to compensate the fiber induced noise.

### 3.2. JGN2plus optical fiber link

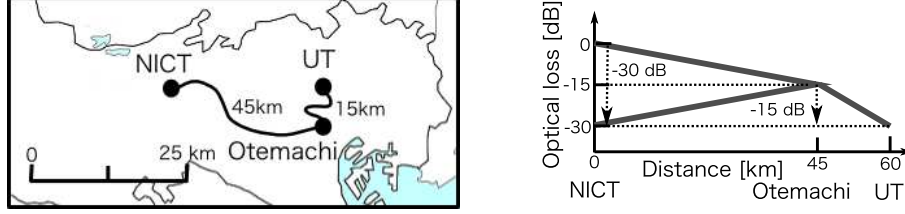


Fig. 3. Schematic diagram of the optical fiber link in Tokyo (left) and the optical losses (right).

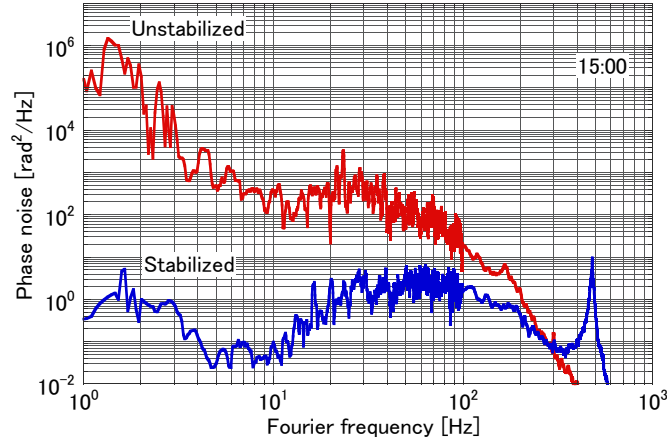


Fig. 4. Phase noises of the out-of-loop beat in the 90-km unstabilized (red) and stabilized (blue) links. The difference of 56 dB at 1 Hz agrees with the theoretical limit of phase noise suppression. Thus, the optical carrier system works properly.

NICT operates an optical fiber network test bed named JGN2plus, as infrastructure for research and development on information and communications technology [14]. Part of the test bed connects NICT and Otemachi (a business district in Tokyo) 45 km away by interconnecting several sections of single-mode dark fiber. To characterize the phase noise cancellation system, we used two parallel links, and joined them at Otemachi so that the local and remote sites of a 90-km link are both at NICT. Fig. 3 shows a schematic diagram of the link. The optical loss is -30 dB for the round-trip link. Fig. 4 depicts the power spectral density of the phase noise imposed on the  $1.5 \mu\text{m}$  light traveling in the round-trip 90-km optical fiber link. This phase noise is much larger than the noises in other optical fiber links [15, 16]. For example, Terra et al. [10] reported phase noise of about  $200 \text{ rad}^2/\text{Hz}$  at a Fourier frequency of 1 Hz in a 480-km link, which is 30 dB less than that in the JGN2plus link. The large amount of noise is probably due to almost half of the link between NICT and Otemachi being buried along a subway line and about one third being wired in the air. This speculation is born out by the fact that the phase noise increases on windy days and decreases at nighttime when the subway is out of service. In addition, the SOP of the transferred light changes dynamically during the transmission because of deformation of the optical fiber core due to temperature and pressure variations. Stable

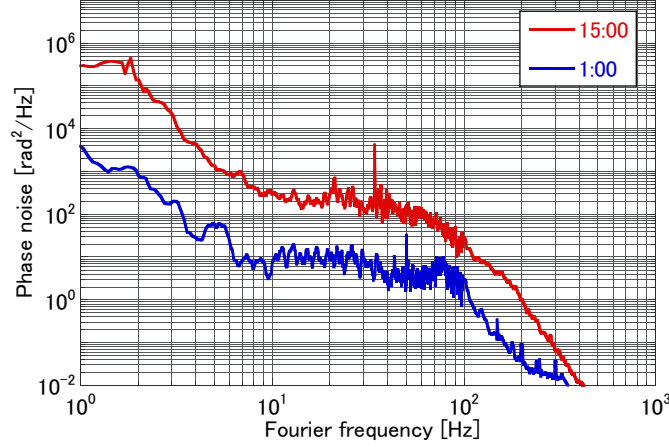


Fig. 5. Phase noise of the 60-km unstabilized link between NICT and UT. The data were obtained at 1:00 and 15:00. The difference between the daytime and nighttime results is one or two orders of magnitude.

transfer of the frequency standard signal requires not only compensation of a huge amount of phase noise but also active polarization control.

NICT was connected to UT by a fiber link with a total length of 60 km by extending the optical fiber link from Otemachi to UT for 15 km. The physical distance between the two laboratories is 24 km. The optical loss in the additional 15 km is -15 dB. This relatively large optical loss is due to the fiber connectors in the multiply-connected link. Fig. 5 shows the power spectral density of the phase noises accumulated on the 60-km NICT-UT link. They were computed from measurements on light traveling in the free-running round-trip NICT-UT-NICT link of 120 km. The level is almost the same as that of the 45-km link, indicating that the path between NICT and Otemachi predominantly induces the phase noise. We evaluated the system in the 90-km link and used this evaluation to estimate the upper limit of the system performance for the 60-km link.

### 3.3. Performance of the optical carrier transfer system

The out-of-loop signal is evaluated by mixing with the reference light, where a 1538-nm fiber laser is used as a light source. The phase noise of the out-of-loop signal was measured as shown in Fig. 4. The blue and red curves show results with and without link stabilization, respectively. These results were obtained at 15:00 in the daytime. The delay of propagation gives limitations of the servo loop bandwidth, which constrains the loop gain of the servo to a finite value. The theoretical maximum of noise suppression is represented as  $1/3(2\pi f\tau)^2$  [4], where  $f$  is the Fourier frequency and  $\tau$  is the one-way propagating time. The maximum cancellation is 56 dB in 90-km links at a Fourier frequency of 1 Hz. As seen in Fig. 4, the suppression ratio reaches the theoretical limit. The bump at 470 Hz found in the stabilized link shows the servo bandwidth for phase locking. Fig. 6 depicts the frequency stability of the out-of-loop signal. It is known that  $\Lambda$ -type frequency counters with a dead time cannot produce the appropriate slope of  $\tau^{-1}$  in the Allan deviation when a signal with white phase noise is counted [17]. We show the results obtained with a  $\Pi$ -type counter (green) as well as with a  $\Lambda$ -type counter (blue). The dashed and solid lines respectively show the stabilities measured from 15:00 to 17:00 in the daytime, and from 1:00 to 3:00 at nighttime. There is an order of difference between the



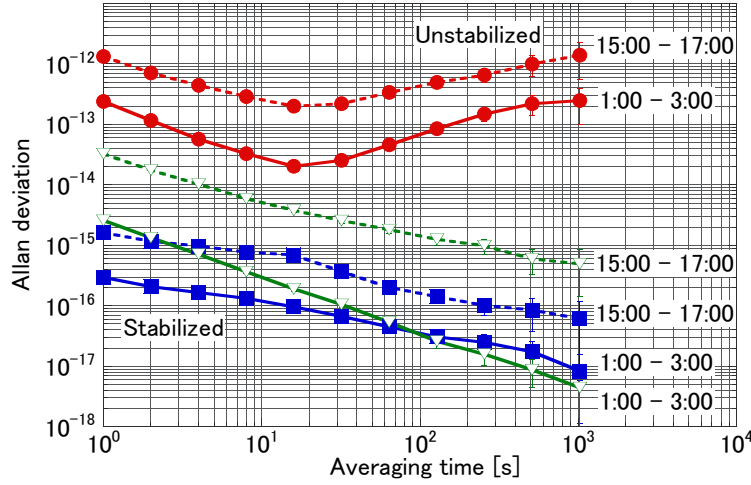


Fig. 6. Frequency stabilities of the transferred signal in the unstabilized (red) and stabilized (blue & green) links. The curves in red and green colors were measured by a  $\Pi$ -type frequency counter. The blue curves were measured by a  $\Lambda$ -type frequency counter. The frequency stabilities shown in the dashed and solid curves were measured during the daytime (15:00-17:00) and around midnight (1:00-3:00), respectively.

short-term stabilities obtained by the  $\Pi$ -type and  $\Lambda$ -type counters. This discrepancy might be attributed to a measurement bandwidth of each frequency counter. At nighttime, the transfer stability measured by a  $\Pi$ -type counter has the  $\tau^{-1}$  slope, resulting in a stability of  $4 \times 10^{-18}$  for an averaging time of 1000 seconds. On the other hand, the transfer stability in the daytime has  $\tau^{-1/2}$  slope, although it was measured with a  $\Pi$ -type counter. This results from the noise component of the unstabilized link in the daytime. As shown in Fig. 4, the phase noise of the unstabilized link has the dependence close to  $1/f^4$  between 1 Hz and 10 Hz. Since fiber noise cancellation follows an  $f^2$  law [4], the slope of the residual phase noise during the daytime is approximately  $1/f^2$  in the stabilized link. Consequently, the stabilized link shows a  $\tau^{-1/2}$  trend like a signal dominated by white FM noise. At nighttime, the fiber noise changes form to a  $1/f^3$  dependence, resulting in a  $\tau^{-1}$  slope. This large difference between daytime and nighttime is attributed to the activity of the subway in Tokyo which is out of service at midnight. In spite of the huge phase noise in the JGN2plus link, the transfer stability reached the  $10^{-18}$  level at nighttime, which is much more stable than a conventional satellite-based link. Additionally, the observed mean deviation of the transferred carrier frequency was  $\Delta\nu = (-2.0 \pm 0.4)$  mHz for the measurement from 1:00 to 3:00 at nighttime, which was within the statistical uncertainty.

### 3.4. Bridge between clock transition and telecom wavelength

#### 3.4.1. Active polarization control and reliable measurement

The conversion efficiency of PPLN is quite sensitive to the SOP of the input light. Hence, active polarization control is essential for reliable measurements without interruption. Our automatic polarization control system based on a commercial polarization tracker is designed to distinguish the signal in the input light from false components caused by reflections from return light at connectors and splices. Fig. 7 shows the schematic diagram of the polarization control system. The out-of-loop signal is coupled to the PPLN through the polarization tracker and the EDFA. The SOP variation due to the EDFA is also compensated in this system. The intensity

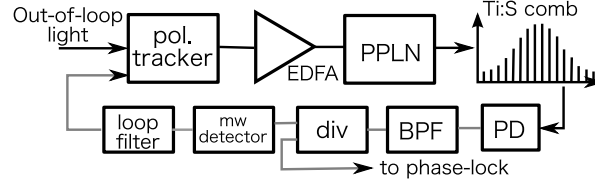


Fig. 7. Schematic diagram of the polarization control system. The polarization variation is detected by the beat intensity between the SHG light and the relevant Ti:S comb component. The rotation is compensated at the polarization tracker (pol. tracker). PPLN: periodically poled lithium niobate, div: divider, BPF: band-pass filter, mw: microwave.

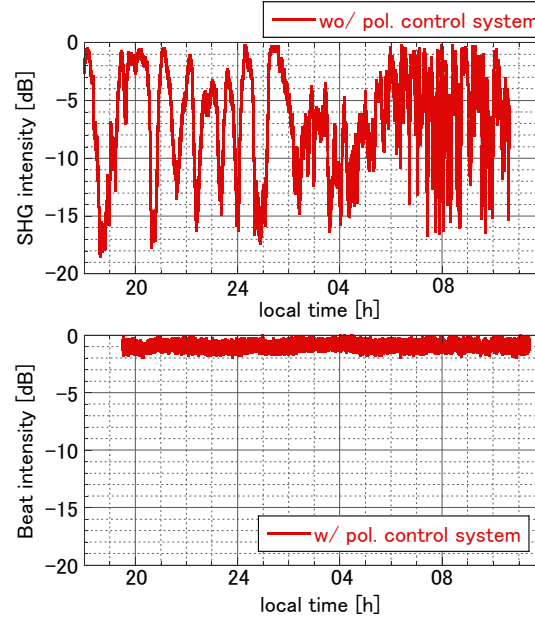


Fig. 8. Up: Intensity variation of the SHG light without the polarization control system. Down: Intensity variation of the beat signal with the polarization control system. Both results were obtained in the 90-km link.

of the correct component of the SHG light is identified as the RF amplitude of the specific beat frequency against the Ti:S frequency comb. The output SHG light is down-converted to the RF domain by the beat detection, where the beat note with the desired component is selectively obtained by a narrow band-pass filter. The intensity is detected with a microwave detector (a planar doped barrier detector). The commercial polarization tracker controls the SOP of the light by driving a fiber squeezer so that the deviation of the feedback signal is reduced. The tracking speed is  $47\pi/\text{s}$ , and the typical SOP recovery time is 0.7 ms, which is fast enough to cancel out the SOP variation in the dedicated link. Fig. 8 shows the behaviors of the intensity fluctuations of the beat signal and SHG light with and without the polarization control system in the 90-km optical fiber link. The results show that the system significantly reduced the intensity fluctuation due to the polarization variation and kept the intensity fluctuation of the beat signal within 2 dB for 16 hours. This novel system is thus capable of continuous operation without manual polarization adjustments. However, a small intensity fluctuation remained even though



the SOP is effectively stabilized by our polarization control system. If an intensity fluctuating signal were sent to a frequency counter, it might induce incorrect readouts in the frequency measurement. To notice such a frequency miscount, the Ti:S frequency comb at the remote site is phase-locked to the SHG light, and the in-loop beat signal between the transmitted signal and the Ti:S frequency comb is counted to confirm a stable phase lock. Note that the Ti:S frequency comb was sometimes phase-unlocked due to the intensity variation of the SHG light before installation of the polarization control system. Thanks to our robust system, the stable intensity of the final beat signal between the Ti:S frequency comb and the clock laser at the remote site helps the frequency counter to read out infallible and reliable values.

#### 3.4.2. Evaluation of instabilities induced by other components

To connect an optical transition in the visible light without a performance degradation, the transfer stabilities of components to bridge the clock lasers and 1.5  $\mu\text{m}$  to be transferred should be lower than the fractional instability of the optical clock. The most critical component is the EDFA. The length variation of the fiber components constituting the EDFA or the amplified spontaneous emission (ASE) noise causes additional phase noise. In our system, a booster EDFA and preamplifier EDFA are used before and after the optical carrier transfer system to compensate for the large optical loss in the urban link. Their performances were evaluated by independent measurements using a fiber interferometer that had arms with and without the device under test, and the relative phase instability was measured using the heterodyne beat. Since the preamplifier EDFA was coupled with the PPLN, the fiber-pigtailed PPLN was also evaluated together with the EDFA. The results of the two instability measurements with a  $\Lambda$ -type counter are depicted in Fig. 9 as curves (a) and (b). The stabilities of the out-of-loop signal and the system noise of the interferometer are depicted as curves (c) and (e), respectively. Since the resultant instabilities of (a) and (b) were in similar level, we concluded that the SHG process with the PPLN did not degrade the frequency stability. Another concern was the phase noise originating from the polarization tracker; however, the results showed that our active polarization control system neither degraded the frequency stability nor gave any frequency offset. In addition, the Ti:S frequency combs at both sites and the ECDL at the local site are tightly phase-locked to the reference light, and their influences are negligibly small. Taking into account all relevant fractional instabilities, the overall instability of the all-optical link system can be expressed as the root sum square of curves (a), (b) and (c) (curve (d)).

### 4. Demonstration of direct comparison of two optical clocks

We tested our novel all-optical link system for making a direct comparison of distant optical clocks through a 60-km urban fiber link in Tokyo. The  $^{87}\text{Sr}$  lattice clocks developed at NICT and UT were compared. The details of the clocks and the Ti:S frequency comb can be found in [18, 19, 20, 21, 22]. The frequency information was sent from NICT to UT, and the fiber noise compensation was done at NICT. The beat note representing the differential clock frequency was measured at UT. The total stability, including those of the clocks and the overall system, is depicted in curve (f) of Fig. 9. The frequency measurement was done with a  $\Lambda$ -type counter around midnight. The short term stability of  $5 \times 10^{-15}$  at 1 second was dominated by the 698-nm clock laser at NICT. Fig. 9 indicates that the all-optical link system does not put any restrictions on the frequency comparison. The system with the 60-km urban fiber link enabled us to determine the relative stability of optical clocks that were 24-km distant from each other. Moreover, after correction of the uncommon systematic shifts, the difference shrank to less than 0.1 Hz with an uncertainty of 0.3 Hz attributed to the lattice clocks, not the fiber link [21]. Additionally, a Hz-level frequency difference between the clocks is clearly visible over the time scale of minutes.

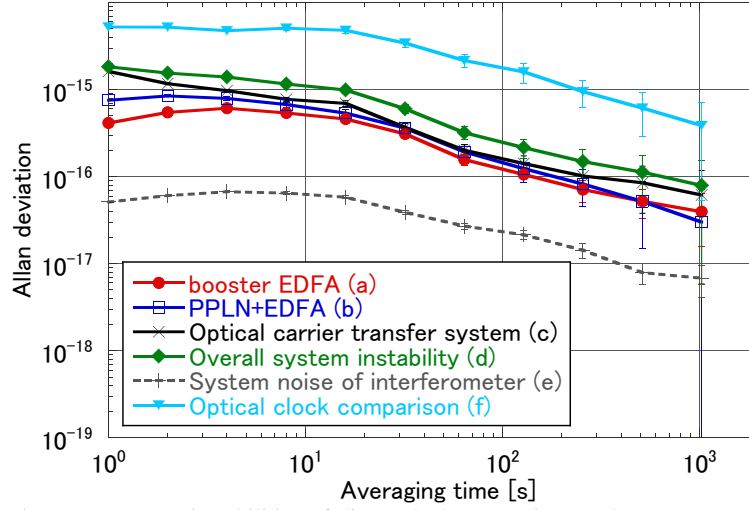


Fig. 9. Frequency instabilities of direct clock comparison and system as measured by a  $\Lambda$ -type counter. The instability of optical clock comparison (f) is not limited by the overall instability (d) of the all-optical link.

## 5. Conclusion

We established an all-optical link connecting two distant optical clocks. A  $1.5\text{-}\mu\text{m}$  light was stably transferred through a 90-km urban fiber link by using an optical carrier transfer system. The transfer stability was  $2 \times 10^{-15}$  at 1 second and  $4 \times 10^{-18}$  at 1000 seconds. A polarization control system for the transmitted light was developed to stabilize the intensity of second harmonic light, enabling long-term and reliable measurements. The overall system instability, including the instabilities of two EDFAs out of the phase-noise compensated path, was  $2 \times 10^{-15}$  at 1 second and  $7 \times 10^{-17}$  at 1000 seconds. The direct comparison of the two  $^{87}\text{Sr}$  lattice clocks was realized in the  $10^{-16}$  uncertainty with the system developed here. The instability of the comparison was not limited by the overall instability of the all-optical link.

The short-term stability of optical clocks has recently improved to the  $10^{-16}$  level [23]. When such stable optical clocks are to be compared, we should use a tracking laser working as low-noise high gain amplifier instead of the uni-directional EDFA employed in the current setup. Moreover, a noise-less optical fiber link would facilitate more stable transfers.

## Acknowledgments

The authors would like to thank Tetsushi Takano, Masao Takamoto and Hidetoshi Katori at the University of Tokyo for their operation of the  $^{87}\text{Sr}$  clock and fruitful cooperation. The authors would like to thank Kazuhiko Nakamura at NICT for his support on the usage of the JGN2plus optical fiber link as well as Ying Li and Clayton Locke at NICT for their cooperation. This work was supported by the JSPS through its FIRST program.